

## Research Article

# Research of Jiles-Atherton Dynamic Model in Giant Magnetostrictive Actuator

**Yongguang Liu, Xiaohui Gao, and Chunxu Chen**

*School of Automation Science and Electrical Engineering, Beihang University, Beijing 100191, China*

Correspondence should be addressed to Xiaohui Gao; [hgaoxiaohui@126.com](mailto:hgaoxiaohui@126.com)

Received 18 March 2016; Revised 29 July 2016; Accepted 9 August 2016

Academic Editor: Xiao-Qiao He

Copyright © 2016 Yongguang Liu et al. This is an open access article distributed under the Creative Commons Attribution License, which permits unrestricted use, distribution, and reproduction in any medium, provided the original work is properly cited.

Due to the existence of multicoupled nonlinear factors in the giant magnetostrictive actuator (GMA), building precise mathematical model is highly important to study GMA's characteristics and control strategies. Minor hysteresis loops near the bias magnetic field would be often applied because of its relatively good linearity. Load, friction, and disc spring stiffness seriously affect the output characteristics of the GMA in high frequency. Therefore, the current-displacement dynamic minor loops mathematical model coupling of electric-magnetic-machine is established according to Jiles-Atherton (J-A) dynamic model of hysteresis material, GMA structural dynamic equation, Ampere loop circuit law, and nonlinear piezomagnetic equation and demonstrates its correctness and effectiveness in the experiments. Finally, some laws are achieved between key structural parameters and output characteristics of GMA, which provides important theoretical foundation for structural design.

## 1. Introduction

Giant magnetostrictive materials (GMM) are widely used in transducer, precision actuator, and active vibration [1–3] because of large magnetostrictive coefficient, excellent dynamic characteristic, and high energy density. When they are applied in high frequency, establishing accurate mathematical model is crucial to improving controllability and stability [4, 5]. J-A model is established based on magnetization principle by Jiles and Atherton, which has a wide application and fast development because of clear physical conception, high stability, and accuracy [6–9]. In recent years, many experts established the mathematical models of hysteresis materials including frequency, pressure, temperature, and other sensitive factors based on the J-A model that had developed a relatively mature modeling theory [10–13]. However, these modes of GMA are mainly studied from material and ignore the structural factors such as load, disc spring stiffness, and friction which have a strong impact on output characteristics especially in high frequency. Therefore, a new dynamic model including load, disc spring stiffness, and friction is established based on combination of minor

loops J-A model of GMM, structural dynamic equation of GMA, Ampere circuit law, and nonlinear piezomagnetic equation through analyzing the working principle of GMA. Then, the correctness and validity of this model are proved by experiments in different conditions. Finally, some output characteristics laws are revealed by analyzing key structural parameters.

## 2. Working Principle of GMA

The GMM rod drives load under the action of the magnetic field generated by the excitation coil and permanent magnet (Figure 1). The magnetostrictive coefficient of GMM is raised by prepressure which is generated by compressing disc spring. Bias magnetic fields are produced by permanent magnets. On the one hand, the double frequency characteristic of GMM could be removed; on the other hand, the high linearity part of hysteresis loop near the bias magnetic fields is applied to reduce the nonlinearity. The temperature control system provides relatively constant temperature environment for the GMM rod.

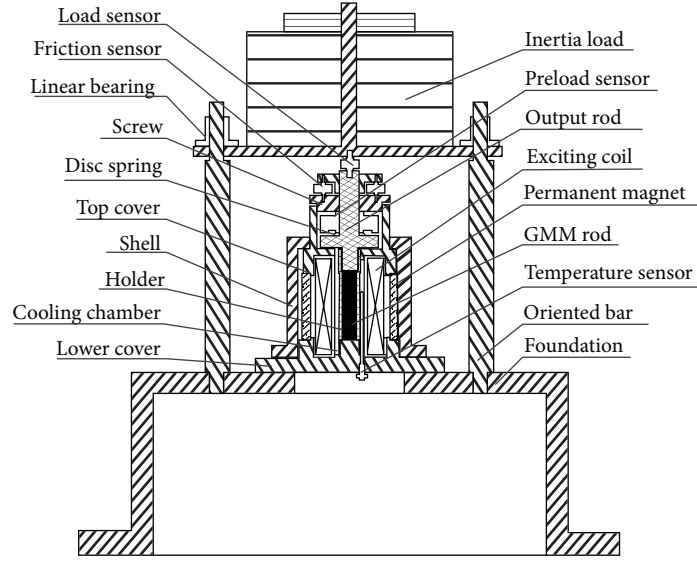


FIGURE 1: Structure of GMA.

### 3. Jiles-Atherton Dynamic Model

The J-A model is developed taking into account the phenomenology of domain wall translation through the so-called pinning center, which might be nonmagnetic inclusions and impurities, grain boundaries, voids, and so forth, causing residual stress that hinders the magnetization process [14]. The motion of magnetic domains can be divided into reversible or irreversible movement and rotation. Thus, according to model developers, total magnetization  $M$  can be divided into reversible and irreversible terms [6]. Hence,

$$M = M_{\text{rev}} + M_{\text{irr}}, \quad (1)$$

where  $M_{\text{rev}}$  is reversible magnetization and  $M_{\text{irr}}$  is irreversible magnetization. Consider

$$\begin{aligned} M_{\text{rev}} &= c(M_{\text{an}} - M_{\text{irr}}), \\ M_{\text{irr}} &= \frac{(M - cM_{\text{an}})}{(1 - c)}, \end{aligned} \quad (2)$$

where  $c$  is reversible loss coefficient.

The modified Langevin equation is used to fit the isotropic material and anhysteretic magnetization  $M_{\text{an}}$  is obtained in

$$M_{\text{an}} = M_s \left( \coth \frac{H + \alpha M_{\text{an}}}{a} - \frac{a}{H + \alpha M_{\text{an}}} \right), \quad (3)$$

where  $M_s$  is saturation magnetization,  $a$  is shape parameter of the anhysteretic magnetization,  $\alpha$  is internal coupling field coefficient among different magnetic domains, and  $H$  is magnetic strength.

Equation (4), which takes into account dynamic effects due to eddy currents in the material, is derived by introducing additional energy term in the basic J-A equation [15]. Hence,

$$\begin{aligned} M &= M_{\text{an}} - k\delta(1 - c) \frac{dM_{\text{irr}}}{dH_e} - k_1 \frac{dM}{dt} \frac{dM}{dH_e} \\ &\quad - k_2 \left| \frac{dM}{dt} \right|^{1/2} \frac{dM}{dH_e}, \end{aligned} \quad (4)$$

where  $k_1$  is eddy-current loss factor,  $k_2$  is anomalous loss factor,  $k$  is irreversible loss coefficient,  $H_e$  is effective magnetic field strength, and  $\delta$  is direction coefficient, when  $dH/dt > 0$ ,  $\delta = 1$  and when  $dH/dt < 0$ ,  $\delta = -1$ .

Stress can change certain features of some magnetic domains to influence  $H_e$ . When the stress is  $\sigma$ , the effective magnetic field  $H_e$  becomes formula (5) and parameter  $\alpha$  is modified to be  $\tilde{\alpha}$  [16, 17]. Hence,

$$H_e = H + \alpha M + \frac{9\lambda_s \sigma}{2\mu_0 M_s^2} M = H + \tilde{\alpha} M, \quad (5)$$

$$\tilde{\alpha} = \alpha + \frac{9\lambda_s \sigma}{2\mu_0 M_s^2}, \quad (6)$$

where  $\lambda_s$  is saturation magnetostrictive coefficient.

According to parameters characteristics of J-A model and the difference between simulation and experiment, the minor loop J-A model can be got through modifying the parameters  $a$ ,  $\alpha$ ,  $c$ , and  $k$  [18]. Hence,

$$\begin{aligned} a_{\text{minor}} &= ae^{\gamma_a(\lambda_s - \lambda_m)}, \\ \alpha_{\text{minor}} &= \alpha e^{\gamma_\alpha(\lambda_s - \lambda_m)}, \\ c_{\text{minor}} &= ce^{\gamma_c(\lambda_s - \lambda_m)}, \\ k_{\text{minor}} &= ke^{\gamma_k(\lambda_s - \lambda_m)}, \end{aligned} \quad (7)$$

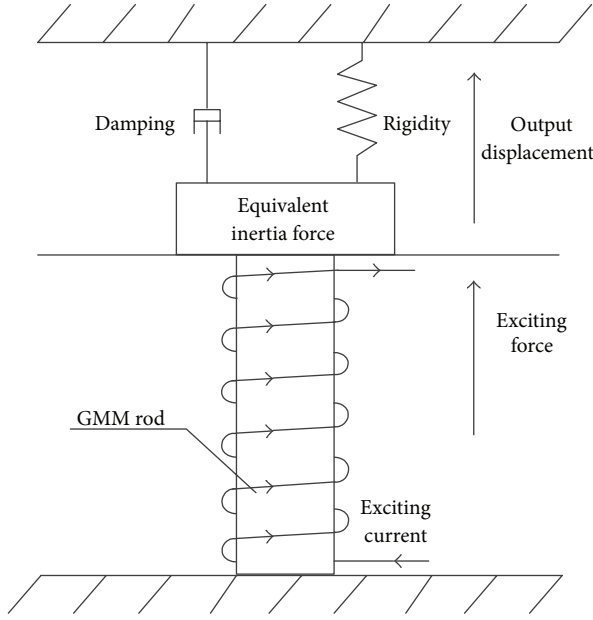


FIGURE 2: Equivalent mechanical mode.

where  $\gamma_k$ ,  $\gamma_a$ ,  $\gamma_c$ , and  $\gamma_\alpha$  are, respectively, modified coefficient of  $k$ ,  $a$ ,  $c$ , and  $\alpha$ ;  $\lambda_m$  is the maximum magnetostriction coefficient of minor loop.

We can get dynamic minor loop J-A model of GMM according to formulas (1)–(7).

#### 4. Structural Dynamics Model

GMA can be considered as a single degree of freedom mass-spring-damping system. GMM rod drives the load under the action of magnetic field. In this section, the dynamic mathematical model of GMA is established considering structural characteristics such as load, disc spring, and friction and the following assumptions should be accepted:

- (1) GMM rod should be in uniform magnetic field.
- (2) The working temperature is 293 K and remains constant all the time.
- (3) The output displacement is 0 when bias magnetic field is 22.5 kA/m, and prepressure is 6 Mpa.
- (4) The output displacement of one end is 0, while the other end keeps the same output characteristics with load such as displacement, velocity, and acceleration.
- (5) The output displacement  $x$  of GMM rod is equal to  $\varepsilon L$  and the output force  $F$  is equal to  $-\sigma A$ .

Based on the above assumptions, the equivalent mechanical mode can be obtained according to the working principle of GMA (Figure 2). According to Newton's second law, the output force  $F$  of GMA is

$$F = -\sigma A = M_e \ddot{x} + C_M \dot{x} + F_f + F_d, \quad (8)$$

$$M_e = \frac{M_M}{3} + M_L,$$

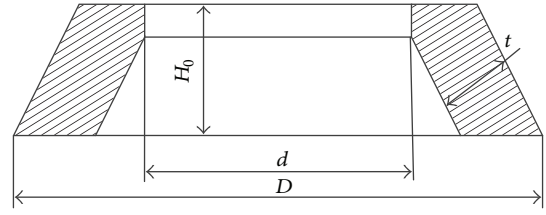


FIGURE 3: Structural parameters of disc spring.

where  $M_e$  is equivalent mass,  $C_M$  is the impedance factor of GMA,  $F_f$  is friction,  $F_d$  is the pressure of disc spring,  $M_M$  is the quality of GMM bar that is equal to 1/3 of itself according to kinetic energy Lagrange function [19], and  $M_L$  is mass of the load.

**4.1. The Output Force of GMM Rod.** When the magnetic field intensity is relatively large, the magnetization process in the material will produce serious hysteresis nonlinearity. The quadratic magnetic domain rotation model is introduced into the linear piezomagnetic equation [20]. Hence,

$$\varepsilon = \frac{\sigma}{E} + \gamma_1 M^2, \quad (9)$$

where  $\gamma_1$  is the magnetic elastic coefficient of GMM rod and  $E$  is the elasticity modulus of GMM rod.

**4.2. Pressure of Disc Spring.** The pressure generated by a single disc spring [21] is given by

$$F_d = \frac{(x + x_0) t^3}{\chi D^2} \left[ \left( \frac{h_0}{t} - \frac{(x + x_0)}{t} \right) \cdot \left( \frac{h_0}{t} - \frac{(x + x_0)}{2t} \right) + 1 \right] - \sigma_0 A, \quad (10)$$

where  $\sigma_0$  is the prestress,  $x_0$  is the predisplacement in the prestress,  $\chi$  is shape factor of disc spring, and  $h_0$  is its maximum deformation. The geometric parameters are shown in Figure 3.

**4.3. Friction.** According to principle and characteristics of friction and working environment of GMA, Coulomb + Viscosity friction model (Figure 4) is selected [22].

Friction model is shown in

$$F_f = f_c v + f_{\max} \operatorname{sgn}(v), \quad (11)$$

where  $f_{\max}$  is the maximum static friction,  $f_c$  is the Coulomb friction coefficient, and  $v$  is velocity of the GMM rod.

**4.4. Ampere Circuital Theorem.** According to Ampere circuital theorem considering leakage in magnetic circuit [23], the magnetic field strength  $H$  is

$$H = H_{\text{bias}} + k_{\text{coil}} I, \quad (12)$$

where  $H_{\text{bias}}$  is the bias magnetic field strength and  $k_{\text{coil}}$  is exciting coefficient of the coil.

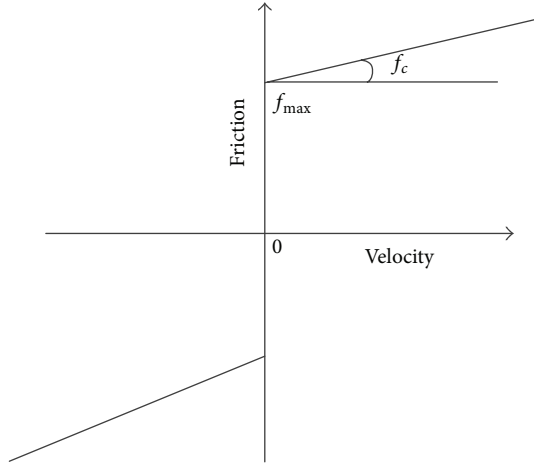


FIGURE 4: Friction model.

TABLE 1: Model parameters.

Parameter	Value
$M_s$	380769 A/m
$k$	22643 A/m
$C_M$	$3.02 \times 10^4$ Ns/m
$\lambda_s$	1500 ppm
$\gamma_1$	$1.07 \times 10^{-14}$ A <sup>2</sup> /m <sup>2</sup>
$a$	47704 A/m
$c$	0.1
$k_1$	$2.62 \times 10^{-5}$
$\gamma_a$	-10
$\gamma_k$	-30
$\alpha$	0.417
$k_{coil}$	$16492$ m <sup>-1</sup>
$k_2$	0.312
$\gamma_\alpha$	10
$\gamma_c$	1500

The current-displacement mathematical model of GMA could be obtained by connecting formulas (1)–(7) with (9)–(12) and its parameters (Table 1) are identified by adopting modified simulated annealing differential evolution algorithm which has a high convergence speed and accuracy.

## 5. Test Verification

GMA testbed is mainly composed of GMA, laser displacement sensor, and temperature control system (Figure 5). The measurement and control system applies RTX as lower computer system software and LabWindows as upper computer system software and sampling period is 0.5 ms. The temperature sensor is installed near GMM rod (Figure 1) and temperature control system can pass heat through circulating water which can be controlled within 1 K by heater and cooler. The V100-MS laser displacement sensor can measure the

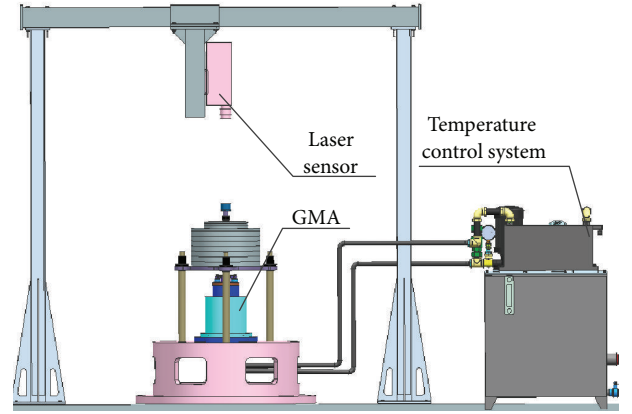


FIGURE 5: GMA testbed.

TABLE 2: Structural parameters of disc spring.

	$D$ (mm)	$d$ (mm)	$t$ (mm)	$h_0$ (mm)
A	63	31	3.5	1.4
B	63	31	2.5	1.75
C	63	31	1.8	2.35

displacement, velocity, and acceleration and its displacement measurement accuracy is up to  $5 \mu\text{m/V}$ . The ISF20DA250 servo driver can provide exciting current with feedback control and its frequency response is up to 15 kHz (see Figure 6). The simulation and experiment curves in different conditions are shown in Figure 7, which prove the validity and accuracy of this mathematical model.

## 6. Studies on Key Parameters of the Model

In this section, the output characteristics laws of GMA are revealed by studying structural parameters such as disc spring stiffness and friction.

**6.1. Studies on Characteristics of Disc Spring.** The disc spring, a key part that provides prepressure, has a serious impact on output characteristics of GMA because of its nonlinearity. This paper studies three series of disc springs (A, B, and C) whose inner and outer diameter are the same and their structural parameters and mechanical property are shown in Table 2 and Figure 8. Figure 9 shows the output displacement of GMA under 20 Hz. After analyzing Figures 8 and 9, we can conclude that the larger stiffness of disc spring can reduce magnetostriction coefficient.

**6.2. Studies on Friction.** This section mainly studies Coulomb friction coefficient  $f_c$  and the maximum static friction  $f_{max}$  in friction model. When  $f_c$  takes 10 Nm/s and 100 Nm/s, respectively, the output displacement of GMA under 20 Hz is shown in Figure 10. The larger the  $f_c$ , the more serious the hysteresis energy loss. As a result, the Coulomb friction coefficient should be as small as possible.

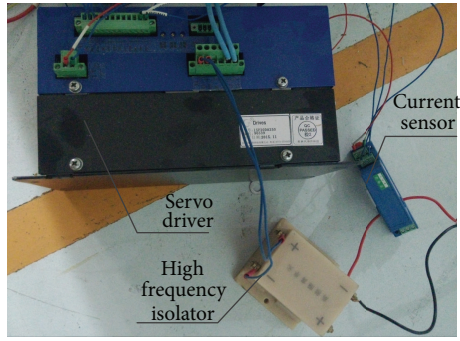


FIGURE 6: Servo driver.

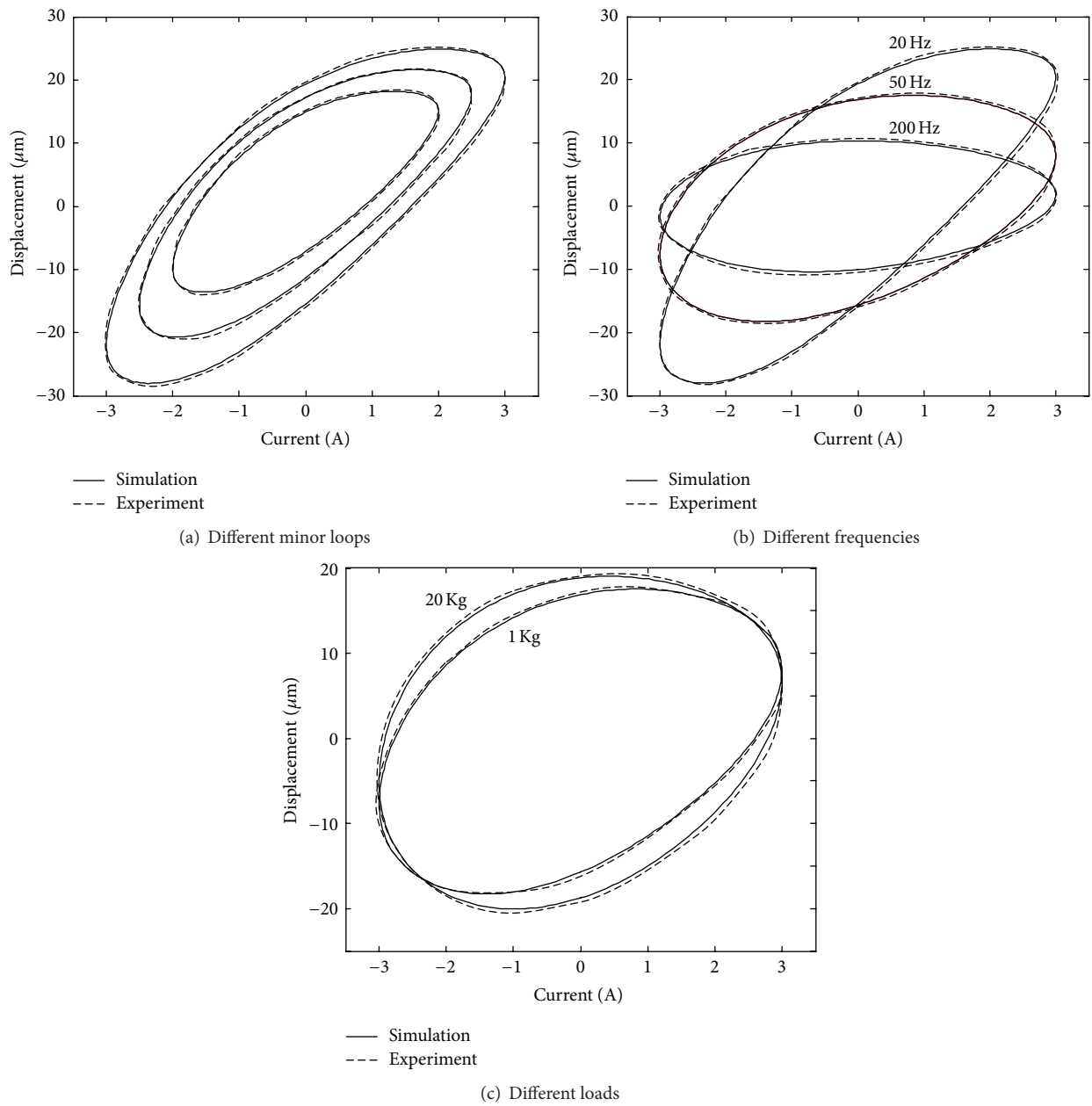


FIGURE 7: Experiment and simulation.

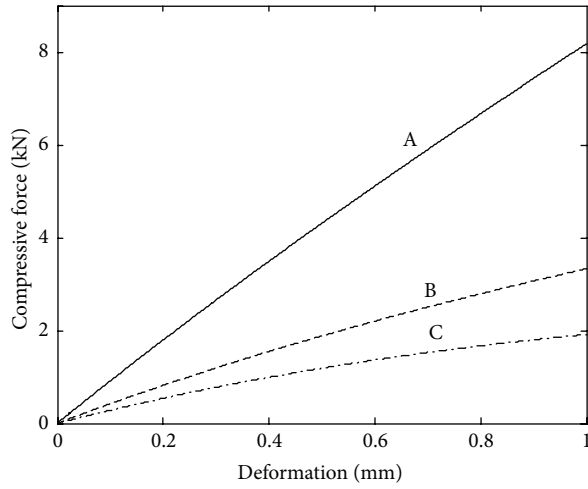


FIGURE 8: Mechanical characteristics curve.

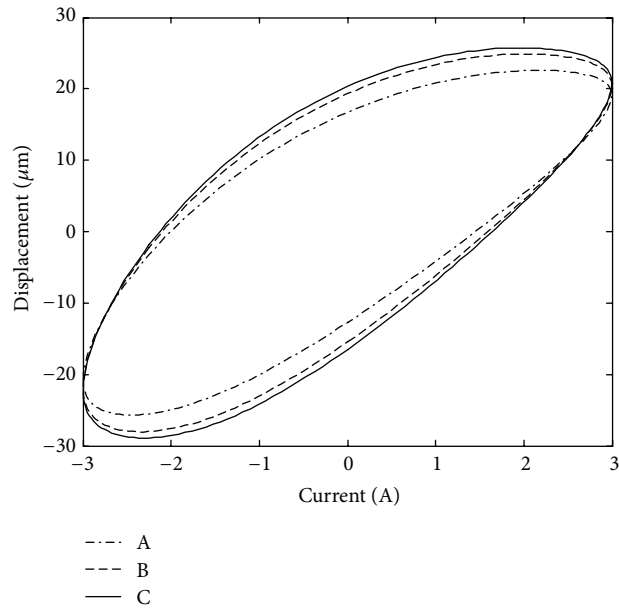


FIGURE 9: Hysteresis loop about springs.

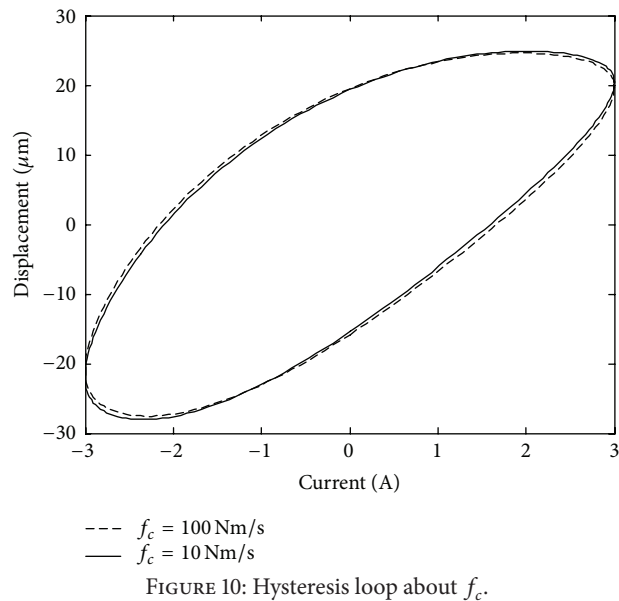


FIGURE 10: Hysteresis loop about  $f_c$ .

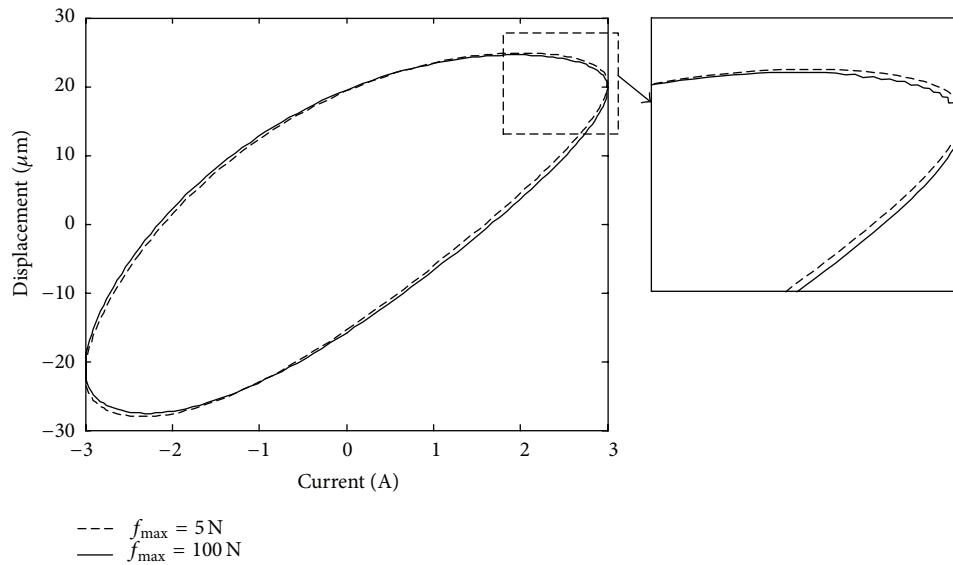


FIGURE 11: Hysteresis loop about  $f_{\max}$ .

When  $f_{\max}$  takes 5 N and 100 N, the output displacement of GMA in 20 Hz is shown in Figure 11. With the increasing of  $f_{\max}$ , serious low speed crawling and buffeting will appear in the end of hysteresis loop. Therefore,  $f_{\max}$  should be as small as possible.

## 7. Conclusion

- (1) Structural parameters have a strong impact on output characteristics of GMA in high frequency.
- (2) The dynamic mathematical model of GMA including structural element such as load, disc spring, and friction has a great adaptability and accuracy.
- (3) The stiffness of disc spring influences the output characteristics of GMA.
- (4) Friction affects unfavourably the output characteristics.

## Competing Interests

The authors declare that they have no competing interests.

## References

- [1] M. R. Karafi, Y. Hojjat, and F. Sassani, "A new hybrid longitudinal-torsional magnetostrictive ultrasonic transducer," *Smart Materials and Structures*, vol. 22, no. 6, Article ID 065013, 2013.
- [2] H. Yoshioka, H. Shinno, and H. Sawano, "A newly developed rotary-linear motion platform with a giant magnetostrictive actuator," *CIRP Annals—Manufacturing Technology*, vol. 62, no. 1, pp. 371–374, 2013.
- [3] F. Braghin, S. Cinquemani, and F. Resta, "A low frequency magnetostrictive inertial actuator for vibration control," *Sensors and Actuators A: Physical*, vol. 180, pp. 67–74, 2012.
- [4] Y. Zhu and Y. Li, "Development of a deflector-jet electrohydraulic servovalve using a giant magnetostrictive material," *Smart Materials and Structures*, vol. 23, no. 11, Article ID 115001, 2014.
- [5] T. Zhang, B. T. Yang, H. G. Li, and G. Meng, "Dynamic modeling and adaptive vibration control study for giant magnetostrictive actuators," *Sensors and Actuators A: Physical*, vol. 190, pp. 96–105, 2013.
- [6] D. C. Jiles and D. L. Atherton, "Theory of ferromagnetic hysteresis," *Journal of Magnetism and Magnetic Materials*, vol. 61, no. 1-2, pp. 48–60, 1986.
- [7] D. C. Jiles, "Frequency dependence of hysteresis curves in conducting magnetic materials," *Journal of Applied Physics*, vol. 76, no. 10, pp. 5849–5855, 1994.
- [8] N. N. Sarawate and M. J. Dapino, "A dynamic actuation model for magnetostrictive materials," *Smart Materials & Structures*, vol. 17, no. 6, Article ID 065013, pp. 1–6, 2008.
- [9] K. Chwastek, "Modelling of dynamic hysteresis loops using the Jiles-Atherton approach," *Mathematical and Computer Modelling of Dynamical Systems*, vol. 15, no. 1, pp. 95–105, 2009.
- [10] A. Ladjimi and M. R. Mékideche, "Modeling of thermal effects on magnetic hysteresis using the Jiles-Atherton model," *Przeład Elektrotechniczny*, vol. 88, no. 4, pp. 253–256, 2012.
- [11] O. Messal, F. Sixdenier, L. Morel, and N. Burais, "Temperature dependent extension of the jiles-atherton model: study of the variation of microstructural hysteresis parameters," *IEEE Transactions on Magnetics*, vol. 48, no. 10, pp. 2567–2572, 2012.
- [12] A. Nouicer, E. Nouicer, and M. Feliachi, "A neural network for incorporating the thermal effect on the magnetic hysteresis of the 3F3 material using the Jiles-Atherton model," *Journal of Magnetism and Magnetic Materials*, vol. 373, pp. 240–243, 2015.
- [13] C. Li and Q. Xu, "Error modification and temperature simulation of J-A model," *Transactions of China Electrotechnical Society*, vol. 29, no. 9, pp. 232–238, 2014.
- [14] S. E. Zirka, Y. I. Moroz, R. G. Harrison, and K. Chwastek, "On physical aspects of the Jiles-Atherton hysteresis models," *Journal of Applied Physics*, vol. 112, no. 4, Article ID 043916, 2012.

- [15] G. Bertotti, "Physical interpretation of eddy current losses in ferromagnetic materials. I. Theoretical considerations," *Journal of Applied Physics*, vol. 57, no. 6, pp. 2110–2117, 1985.
- [16] M. J. Sablik and D. C. Jiles, "Coupled magnetoelastic theory of magnetic and magnetostrictive hysteresis," *IEEE Transactions on Magnetics*, vol. 29, no. 4, pp. 2113–2123, 1993.
- [17] F. T. Calkins, R. C. Smith, and A. B. Flatau, "Energy-based hysteresis model for magnetostrictive transducers," *IEEE Transactions on Magnetics*, vol. 36, no. 2, pp. 429–439, 2000.
- [18] G. Xiaohui, L. Yongguang, and P. Zhongcai, "Minor hysteresis loop dynamic jiles-atherton model in giant magnetostrictive actuator," *Journal of Beijing University of Aeronautics and Astronautics*, 2016.
- [19] T. Zhifeng, *Funfamental Theory and Experiments Study of Giant Magnetostrictive Actuator*, Zhejiang University, Hangzhou, China, 2005.
- [20] S.-Y. Cao, B.-W. Wang, R.-G. Yan, W.-M. Huang, and L. Weng, "Dynamic model with hysteretic nonlinearity for a giant magnetostrictive actuator," *Proceedings of the Chinese Society of Electrical Engineering*, vol. 23, no. 11, pp. 145–149, 2003.
- [21] W. Wenbin, *Machinerys Handbook, Mechanical Design*, China Machine Press, Beijing, China, 2004.
- [22] L. Lila, L. Hongzhao, and W. Ziyingect, "Research progress of friction model in mechanical system," *Advances in Mechanics*, vol. 38, no. 2, pp. 201–211, 2008.
- [23] J. Zhenyuan, W. Xiaoyi, and W. Fuji, "Parameters identification method of Giant Magnetostrictive Actuators," *Chinese Journal of Mechanical Engineering*, vol. 43, 2007.





# Hindawi

Submit your manuscripts at  
<http://www.hindawi.com>

